DESY 96–199
INLO-PUB-20/96
WUE-ITP-96-018
hep-ph/9609400
September 1996

# A Detailed Comparison of NLO QCD Evolution Codes

J. Blümlein, S. Riemersma

*DESY–Zeuthen, Platanenallee 6, D–15735 Zeuthen, Germany*

M. Botje

*NIKHEF, PO Box 41882, 1009 DB Amsterdam, The Netherlands*

C. Pascaud, F. Zomer

*LAL, IN2P3-CNRS et Université de Paris-Sud*
*F–91495 Orsay Cédex, France*

W.L. van Neerven

*Instituut Lorentz , Rijksuniverstiteit Leiden*
*PO Box 9506, 2300 RA Leiden, The Netherlands*

A. Vogt

*Institut für Theoretische Physik, Universität Würzburg*
*Am Hubland, D–97074 Würzburg, Germany*

## Abstract

Seven next-to-leading order QCD evolution programs are compared. The deviations of the results due to different theoretical prescriptions for truncating the perturbative series are clarified, and a numerical agreement between five codes of better than 0.1% is achieved. Reference results for further comparison are provided.

*To appear in the proceedings of the workshop "Future Physics at HERA", DESY, Hamburg, 1996.*

# A Detailed Comparison of NLO QCD Evolution Codes

J. Blümlein[a], M. Botje[b], C. Pascaud[c], S. Riemersma[a],
W.L. van Neerven[d], A. Vogt[e,f], and F. Zomer[c]

[a] DESY-Zeuthen, Platanenallee 6, D–15738 Zeuthen, Germany
[b] NIKHEF, PO Box 41882, 1009 DB Amsterdam, The Netherlands
[c] LAL, IN2P3-CNRS et Université de Paris-Sud, F–91495 Orsay Cédex, France
[d] Instituut Lorentz, Rijksuniversiteit Leiden, PO Box 9506, 2300 RA Leiden, The Netherlands
[e] Deutsches Elektronen-Synchrotron DESY, Notkestraße 85, D–22603 Hamburg. Germany
[f] Institut für Theoretische Physik, Universität Würzburg, D–97074 Würzburg, Germany

**Abstract:** Seven next-to-leading order QCD evolution programs are compared. The deviations of the results due to different theoretical prescriptions for truncating the perturbative series are clarified, and a numerical agreement between five codes of better than 0.1% is achieved. Reference results for further comparison are provided.

## 1 Introduction

In order to exploit the full potential of HERA for deep–inelastic scattering (DIS), the highest possible luminosities and considerable efforts for the reduction of experimental systematic uncertainties are necessary. This will finally allow a measurement of the proton structure function $F_2$ over a wide range, with errors on the level of very few percent [1]. To make full use of such results, and to allow even for combined analyses using the high–precision fixed–target data as well, the structure function evolution programs required for the necessary multi–parameter QCD fits have to be numerically and conceptually under control to a much higher accuracy. At least one order of magnitude is desirable. This accuracy is necessary to safely rule out contributions to the theory error of $\alpha_s(M_Z^2)$ which arise from the particular technical implementation of the solution of the NLO evolution equations. Due to the current apparent difference in $\alpha_s(M_Z^2)$ as determined in $e^+e^-$ and DIS experiments [2], this question is of particular importance for the future QCD analyses based on the HERA structure function data.

So far no high–precision comparison of next-to-leading-order (NLO) programs has been performed including the full HERA range. In previous studies partial comparisons were carried out demanding a considerably lower accuracy (see e.g. ref. [3]). Other comparisons focussed on the valence range and compared the effect of different codes used for the QCD fit on $\Lambda_{\rm QCD}$ only, see ref. [4]. The required accuracy cannot be easily reached by just comparing results to published parametrizations, due to their inaccuracies, caused by respective numerical representations. Often also the physical and technical assumptions made are not fully documented.

In this paper, we present the results of a dedicated effort, comparing the results of seven NLO codes under perfectly controlled conditions. The paper is organized as follows. In Section 2 we recall the basic formulae, and sketch the most commonly used approaches to the evolution equations. Section 3 compares the differences of six 'global' evolution programs. The clarification of the deviations found there, using also a seventh program especially suited for the 'local' evolution of $F_2$, is described in Section 4. The size of the numerical differences which persist after this development is investigated in Section 5, where also reference results for further comparison are provided. Finally Section 6 contains our summary.

# 2 Approaches to the Next-to-Leading Order Evolution

The evolution equations for the parton distributions $f(x, Q^2)$ of the proton are given by

$$\frac{\partial f(x, Q^2)}{\partial \ln Q^2} = \left[ a_s(Q^2)\, P_0(x) + a_s^2(Q^2)\, P_1(x) + O(a_s^3) \right] \otimes f(x, Q^2) \; . \tag{1}$$

Here $x$ stands for the fractional momentum carried by the partons, and $\otimes$ denotes the Mellin convolution. For brevity, we have introduced $a_s(Q^2) \equiv \alpha_s(Q^2)/4\pi$. Eq. (1) is understood to represent, in a generic manner, the non–singlet cases as well as the coupled quark and gluon evolutions. $P^{(0)}$ and $P^{(1)}$ denote the corresponding leading order (LO) and NLO splitting functions, respectively (see, e.g., ref. [5]). Only these two coefficients of the perturbative series are completely known so far, hence the solution of the evolution equations is presently possible only up to NLO. To this accuracy, the scale dependence of the strong coupling $a_s(Q^2)$ reads

$$\frac{\partial\, a_s(Q^2)}{\partial \ln Q^2} = -\beta_0 a_s^2(Q^2) - \beta_1 a_s^3(Q^2) + O(a_s^4) \; . \tag{2}$$

Throughout our comparisons, we will identify the renormalization and factorization scales with $Q^2$, as already indicated in eqs. (1) and (2). For different choices see refs. [6, 7]. Introducing the QCD scale parameter $\Lambda$, the solution of eq. (2) can be written as

$$a_s(Q^2) \simeq \frac{1}{\beta_0 \ln(Q^2/\Lambda^2)} - \frac{\beta_1}{\beta_0^3} \frac{\ln\left[\ln(Q^2/\Lambda^2)\right]}{\ln^2(Q^2/\Lambda^2)} \; . \tag{3}$$

Two approaches have been widely used for dealing with the integro–differential equations (1). In many analyses, they have been numerically solved directly in $x$-space. We will exemplify some techniques applicable in this case for one particular program, choosing 'QCDNUM', which is based on the programs of ref. [8], and is planned to become publicly available [9]. See, for example, ref. [10] for a description of a differing $x$-space implementation.

In QCDNUM, the $Q^2$ evolution of the parton momentum densities is calculated on a grid in $x$ and $Q^2$, starting from the $x$-dependence of these densities at a fixed reference scale $Q_0^2$. The logarithmic slopes in $Q^2$ are calculated from eq. (1). To compute the convolution integrals, the assumption is made that the parton distributions can be linearly interpolated (at all $Q^2$) from one $x$ gridpoint to the next. With this assumption the integrals can be evaluated as weighted sums. The weights, which are essentially integrals over the splitting functions, are numerically calculated (by Gauss integration) to high precision at program initialization. From the value of a given parton distribution and the slopes at $Q_0^2$, the distribution can be calculated at the next gridpoint $Q_1^2 > Q_0^2$ (or $Q_1^2 < Q_0^2$). This distribution then serves to calculate the slopes at $Q_1^2$ etc., and the evolution is continued over the whole $x$–$Q^2$ grid. The evolution algorithm makes use of quadratic interpolation in $\ln Q^2$.

In this way, a fast evolution of parton densities is obtained, entirely based on look-up weight tables which are calculated at program initialization. The numerical accuracy depends on the density of the $x$ grid and, to a lesser extent, on that of the $Q^2$ grid. In the comparisons presented here, 370 gridpoints in $x$ covering $10^{-5} \leq x < 1$ have been used: 230 points distributed logarithmically for $x < 0.2$, and 140 points distributed linearly for $x > 0.2$. A logarithmic $Q^2$ grid with 60 points covered the range $4 < Q^2 < 10^4$ GeV$^2$.

An important alternative to the direct $x$-space treatment, employed in the analyses of refs. [11, 12] based upon ref. [13], is to transform the evolution equations to Mellin-$N$ moments. The main virtue of this transformation is that the convolution is reduced to a simple product. Hence eq. (1) turns into a system of ordinary differential equations at fixed $N$, which allows for an analytic solution. Rewriting the evolution equations in terms of $a_s \equiv a_s(Q^2)$ using eq. (2), and expanding the resulting r.h.s. into a power series in $\alpha_s$, one arrives in NLO at

$$\frac{\partial f(x, a_s)}{\partial a_s} = -\frac{1}{\beta_0 a_s}\left[P^{(0)}(x) + a_s\left(P^{(1)}(x) - \frac{\beta_1}{\beta_0}P^{(0)}(x)\right) + O(a_s^2)\right] \otimes f(x, a_s) \,. \tag{4}$$

After transformation to $N$-moments, its solution can be written down in a closed form for the non–singlet cases, with $a_0 \equiv a_s(Q_0^2)$, as

$$f_N(a_s) = \left[1 - \frac{a_s - a_0}{\beta_0}\left(P_N^{(1)} - \frac{\beta_1}{\beta_0}P_N^{(0)}\right) + O(a_s^2)\right]\left(\frac{a_s}{a_0}\right)^{P_N^{(0)}/\beta_0} f_N(a_0) \,. \tag{5}$$

For the notationally more cumbersome, corresponding relation for the singlet evolution, the reader is referred to refs. [11, 12].

From these analytic solutions, one can acquire the $x$-space results by one contour integral in the complex $N$-plane, see ref. [12]. Using a chain of Gauss quadratures, a numerical accuracy of this integration at better than $10^{-5}$ is readily achieved. In our comparisons, at most 136 fixed support points at complex $N$-values have been used, with this maximal number employed only for very large values of $x$ [14]. Due to the required non–trivial analytic continuations of the NLO anomalous dimensions [12], this approach is technically somewhat more involved than the numerical $x$-space solution. On the other hand, since the $Q^2$ integration is done in one step, regardless of the evolution distance, and the use of fixed support points allows for performing the calculation of the anomalous dimensions only once at program initialization, this method is competitive in speed to the $x$-space iterations.

A partly independent $N$-space program has been developed during this workshop [15], implementing an iterative numerical solution of the Mellin–transformed eq. (4). Since one of the advantages of the $N$-space approach is not exploited here, this program is so far not competitive in speed with the ones discussed before. It has however been of considerable value for cross–checks and theoretical investigations, see below.

Before we now turn to the comparisons, it should be emphasized that a perfect agreement between the results based upon eqs. (1), (4), and (5) is not to be expected, since they all differ in terms of next-to-next-to leading order (NNLO), hidden under the $O(a_s^3)$ and $O(a_s^2)$ signs.

# 3 The Initial Comparisons

All our comparisons are performed under somewhat simplified, but sufficiently realistic conditions. We assume four massless flavours, in eq. (1) as well as in eq. (2), at all scales considered, i.e. effects due the non–zero charm mass and the existence of the bottom quark are not taken into account. All our results below will refer to the $\overline{\mathrm{MS}}$ renormalization and factorization schemes, and the corresponding scales are identified with $Q^2$. The reference scale $Q_0^2$ for the evolution, and the four–flavour QCD scale parameter $\Lambda$ in eq. (3) are chosen as

$$Q_0^2 = 4 \text{ GeV}^2 \; , \quad \Lambda^{(4)}_{\overline{\mathrm{MS}}} = 250 \text{ MeV} \; . \tag{6}$$

The following initial conditions are selected for the (anti-) quark and gluon densities:

$$\begin{aligned} xu_v(x,Q_0^2) &= A_u x^{0.5}(1-x)^3 \; , \; xd_v(x,Q_0^2) \;=\; A_d x^{0.5}(1-x)^4 \; , \\ xS(x,Q_0^2) &= [x\Sigma \,-\, xu_v \,-\, xd_v](x,Q_0^2) \;=\; A_S x^{-0.2}(1-x)^7 \; , \\ xg(x,Q_0^2) &= A_g x^{-0.2}(1-x)^5 \; , \; xc(x,Q_0^2) \;=\; x\bar{c}(x,Q_0^2) \;=\; 0 \; . \end{aligned} \tag{7}$$

The SU(3)–symmetric sea $S$ is assumed to carry 15% of the nucleon's momentum at the input scale, and the remaining coefficients $A_i$ are fixed by the usual sum rules. Finally $F_2$ is determined by simply convoluting the resulting parton densities with the appropriate coefficient functions.

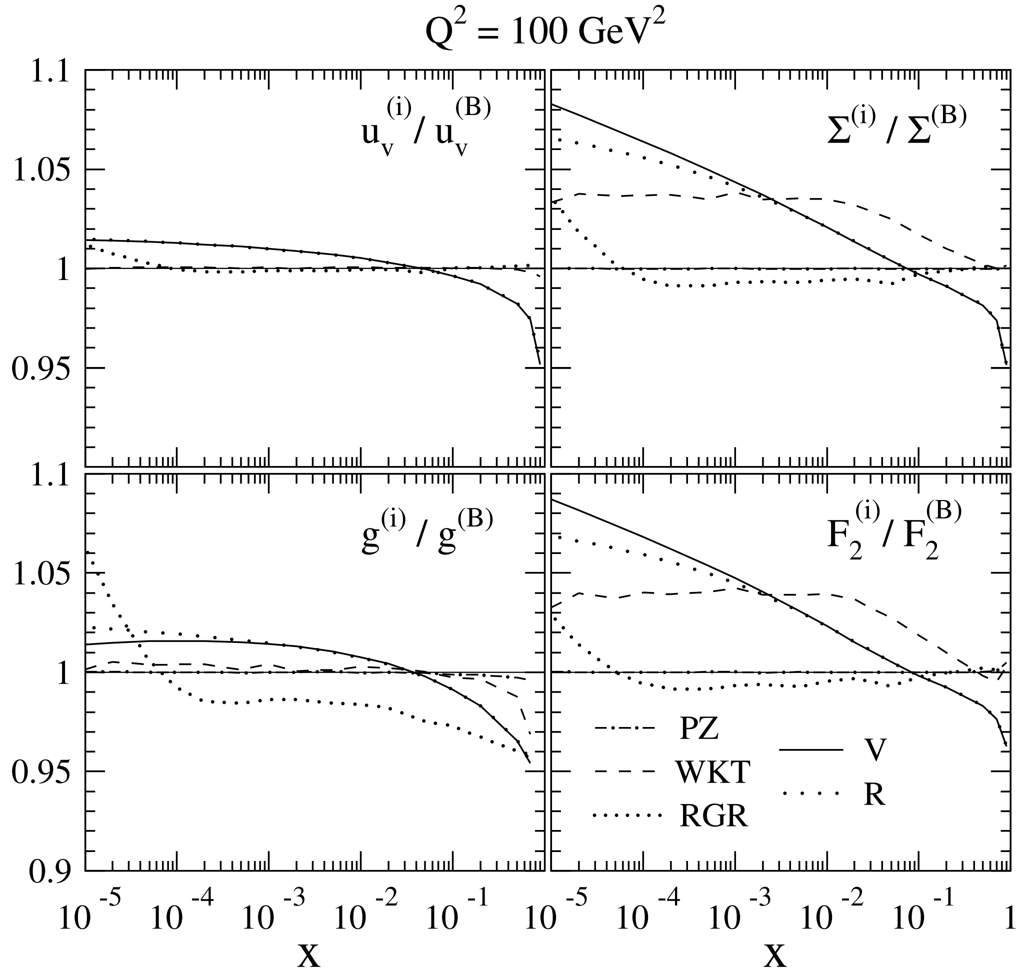


Figure 1: The differences between the up-valence, singlet quark and gluon densities, $u_v$, $\Sigma$ and $g$, and the proton structure functions $F_2$, as obtained from evolving the input (7) with various NLO evolution programs [9, 10, 14, 15, 16, 17] to $Q^2 = 100$ GeV$^2$. All results have been normalized to those of ref. [9]. For a detailed discussion see the text.

The results of our first comparisons are shown in Figure 1. One notices the very good agreement between the programs [9, 10] used by the HERA collaborations. The differences are always much less than 1%, and the curves can hardly be distinguished, except for large $x$, with the present resolution. A similarly excellent agreement is seen between the two $N$-space programs [14, 15], except for very low $x$, where offsets up to 1.5% show up. The most striking feature of the figure, however, is the very sizeable differences between these two groups of programs: the scaling violations, increasing (decreasing) the distributions at small (large) values of $x$, are considerably stronger in the results of refs. [14, 15], although, of course, the same values for $\alpha_s$ are employed as in refs. [9, 10]. This effect reaches a magnitude of as much as 8% for the structure function $F_2$ at the smallest $x$-values considered.

As stated above, perfect agreement had not been expected due to theoretical differences, but the size of this offset was a surprise to most of us. It initiated quite some checking and programming activity, which will be summarized in the next section.

Also shown in the figure are the results obtained by the $x$-space evolution programs of the MRS and CTEQ global fit collaborations [16, 17]. Very good agreement to the results of refs. [9, 10] is found for the valence quarks, except for ref. [16] at extremely low values of $x$. In the singlet sector, however, significant differences are observed for some quantities: 1.5 – 3% on the gluon density in ref. [16], and up to 4% on the sea quark distributions in ref. [17].

# 4 Pinning Down the Differences

Besides checks and comparisons of the numerical values of the NLO splitting between the codes of refs. [9, 14, 15], the large differences discussed in the previous section led to three program developments, which together allowed for their full understanding on an unprecedented level.

- A program for a local representation of the evolution of $F_2$ close to the initial scale, completely independent of all previous ones, was added to the comparisons [18].
- The code of ref. [15] was extended to include, still in moment space, an option for evolving also on the basis of eq. (1) instead of (4).
- The program of ref. [14] was used to simulate an iterative solution of eq. (4) as performed in ref. [15], and additionally two new iterative options, one of them equivalent to eq. (5), were introduced into this package.

The results of these efforts are displayed in Figure 3, where we show the evolution of $F_2$, close to our reference scale $Q_0^2 = 4$ GeV$^2$, for three typical values of $x$. The differences, depicted in the previous figure for $Q^2 = 100$ GeV$^2$, build up very quickly near $Q_0^2$: already around 10 GeV$^2$ they are close to their final level. The second important observation is the perfect agreement of the local representation [18] with the $x$-space codes [9, 10], which immediately stopped any speculations on possible problems in the latter programs. Next one notices that the 1% small-$x$ difference between refs. [14] and [15] is perfectly understood in terms of the slightly different contributions truncated away in eqs. (4) and (5), cf. ref. [6]. The concluding step is the comparison of the modified evolution of [15] with the results of [9, 10, 18]. This reveals that in fact virtually all offsets between the results of refs. [9, 10, 14, 15] in Figure 1 are

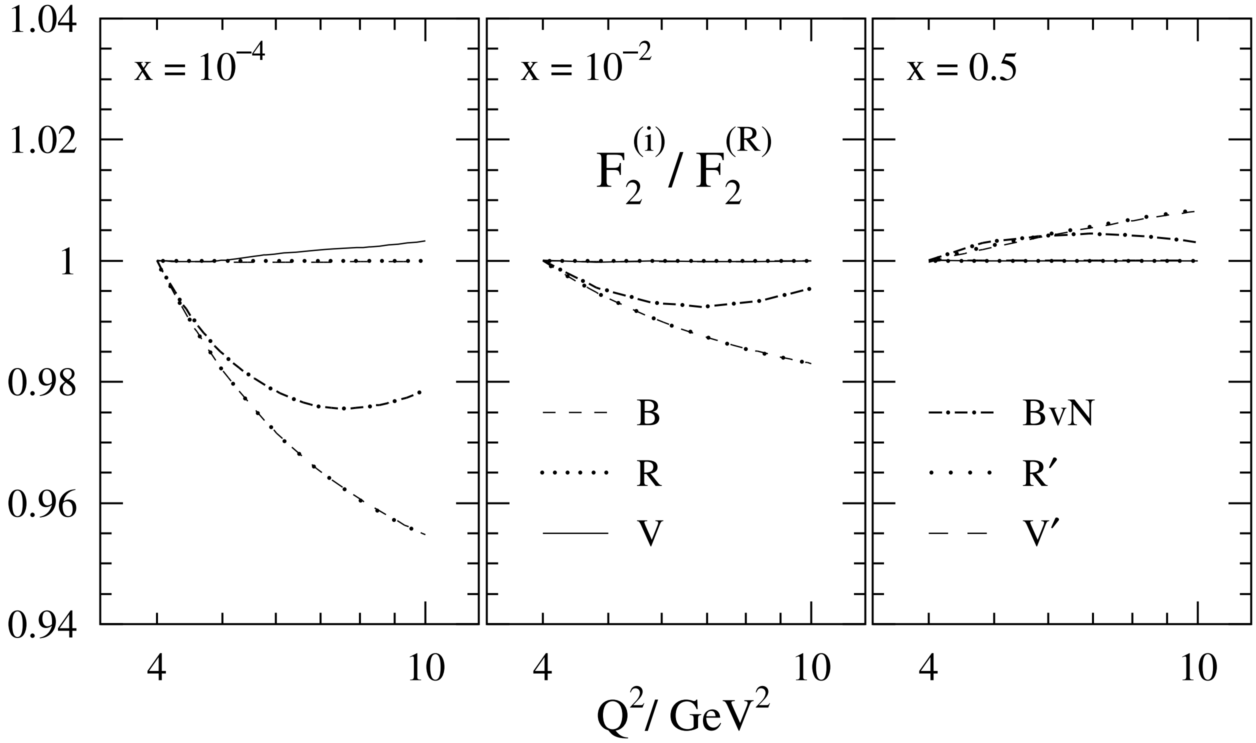


Figure 2: A comparison of results on the $Q^2$ evolution of $F_2$ close to the reference scale $Q_0^2 = 4$ GeV$^2$. The results of refs. [9, 15, 12] (denoted by $\mathbf{B}$, $\mathbf{R}$, and $\mathbf{V}$) are as in the previous figure. $\mathbf{BvN}$ represents a local representation of the $F_2$ evolution [18], and the curves $\mathbf{R}'$ and $\mathbf{V}'$ check the numerical consistency by adapting to the theoretical assumptions of refs. [9] and [15], respectively.

due to the differences introduces by the employed truncation prescriptions for the perturbative series the NLO level, i.e. by terms of NNLO and beyond.

The origin of the differences between the results of refs. [16, 17] and our programs could not be clarified during this workshop. Hence for the very precise comparisons to which we now turn, we will keep only our five program packages, which agree, at least, sizeably better than to 1%.

# 5 The Achieved Numerical Accuracy

Armed now with at least two different codes for any of the truncation prescriptions of Section 2, we can proceed to explore the limits of the agreement of our five program packages under consideration. This complete coverage will be used for comparing all programs, even those with conflicting theoretical treatments, in one figure. For this purpose, the results of refs. [9, 10] have been normalized to the modified evolution of ref. [15] (based upon eq. (1)), whereas the 'iterated' evolution of ref. [14] is normalized to the original results of ref. [15] (based upon eq. (4)).

The results are shown at two fixed $Q^2$ values in Figure 3 for the parton distributions, and in Figure 4 for $Q^2$ evolution of the proton structure function $F_2$ at three fixed values of $x$. The total spread of the results at $Q^2 = 100$ GeV$^2$ amounts to at most about 0.05%, except for very large $x$, where the distributions, especially the gluon density, become very small. Even after evolution to $10^4$ GeV$^2$, the differences are still on the level of 0.1%, meeting the goal formulated in the introduction. Moreover, there is no reason for failing to reach an even higher accuracy, at least to 0.02% as already achieved between the $N$-space programs, also in $x$-space, e.g. by increasing the still not too high number of $Q^2$ grid points in the program of ref. [9].

Finally, for the convenience of those readers who want to check their own existing of forthcoming NLO evolution program to an accuracy well below 0.1% over a wide range in $x$, we show in Table 1 two sets of reference results, which represent the evolution of the initial distributions (7) under the conditions (6), according to eq. (1) and eq. (5) to $Q^2 = 100$ GeV$^2$.

| $x$ | $xu_v$ | $xd_v$ | $xS$ | $2xc$ | $xg$ | $F_2$ |
|---|---|---|---|---|---|---|
| $10^{-5}$ | 9.2793 E-3 | 5.2115 E-3 | 2.6670 E1 | 5.0866 E0 | 9.6665 E1 | 7.0270 E0 |
| $10^{-4}$ | 2.8777 E-2 | 1.6134 E-2 | 1.3862 E1 | 2.4694 E0 | 4.7091 E1 | 3.5868 E0 |
| $10^{-3}$ | 8.7208 E-2 | 4.8678 E-2 | 6.7508 E0 | 1.0663 E0 | 2.0801 E1 | 1.7271 E0 |
| $10^{-2}$ | 2.4598 E-1 | 1.3494 E-1 | 2.8562 E0 | 3.5762 E-1 | 7.5998 E0 | 7.9497 E-1 |
| 0.1 | 4.7450 E-1 | 2.3215 E-1 | 5.7924 E-1 | 4.6496 E-2 | 1.4260 E0 | 3.5397 E-1 |
| 0.3 | 3.1152 E-1 | 1.1662 E-1 | 5.7780 E-2 | 3.5268 E-3 | 1.9173 E-1 | 1.6536 E-1 |
| 0.7 | 2.5048 E-2 | 3.9486 E-3 | 8.0219 E-5 | 4.0111 E-6 | 1.1276 E-3 | 1.4359 E-2 |
| $x$ | $xu_v$ | $xd_v$ | $xS$ | $2xc$ | $xg$ | $F_2$ |
| $10^{-5}$ | 9.4109 E-3 | 5.2848 E-3 | 2.8893 E1 | 5.6465 E0 | 9.8060 E1 | 7.6417 E0 |
| $10^{-4}$ | 2.9144 E-2 | 1.6336 E-2 | 1.4755 E1 | 2.6954 E0 | 4.7859 E1 | 3.8325 E0 |
| $10^{-3}$ | 8.8083 E-2 | 4.9146 E-2 | 7.0516 E0 | 1.1434 E0 | 2.1110 E1 | 1.8094 E0 |
| $10^{-2}$ | 2.4723 E-1 | 1.3553 E-1 | 2.9226 E0 | 3.7584 E-1 | 7.6627 E0 | 8.1358 E-1 |
| 0.1 | 4.7268 E-1 | 2.3097 E-1 | 5.7880 E-1 | 4.7422 E-2 | 1.4152 E0 | 3.5337 E-1 |
| 0.3 | 3.0798 E-1 | 1.1511 E-1 | 5.6817 E-2 | 3.4796 E-3 | 1.8757 E-1 | 1.6349 E-1 |
| 0.7 | 2.4433 E-2 | 3.8429 E-3 | 7.6136 E-5 | 3.5004 E-6 | 1.0854 E-3 | 1.4013 E-2 |

Table 1. Reference results at $Q^2 = 100$ GeV$^2$ for the NLO evolution using the direct solution of eq. (1) (upper half), and the truncated analytic solution (5) (lower half). The initial conditions are specified in eqs. (6) and (7). The estimated numerical accuracy of these results is about 0.02%.

# 6 Summary

The results of seven programs for the NLO evolution of parton densities and structure functions have been compared. Differences due to terms of NNLO, truncated differently in the various implementations, turn out to be larger than anticipated. They can reach, e.g., about 6% at $x = 10^{-4}$ and $Q^2 = 100$ GeV$^2$. A full quantitative understanding of these differences has been achieved at an unprecedented level of accuracy for five of these codes. There the remaining numerical differences are on the level of $\pm 0.02\%$ at $Q^2 = 100$ GeV$^2$. Two sets of reference results, according to different theoretical prescriptions, have been provided for further high-precision checks of evolution programs.

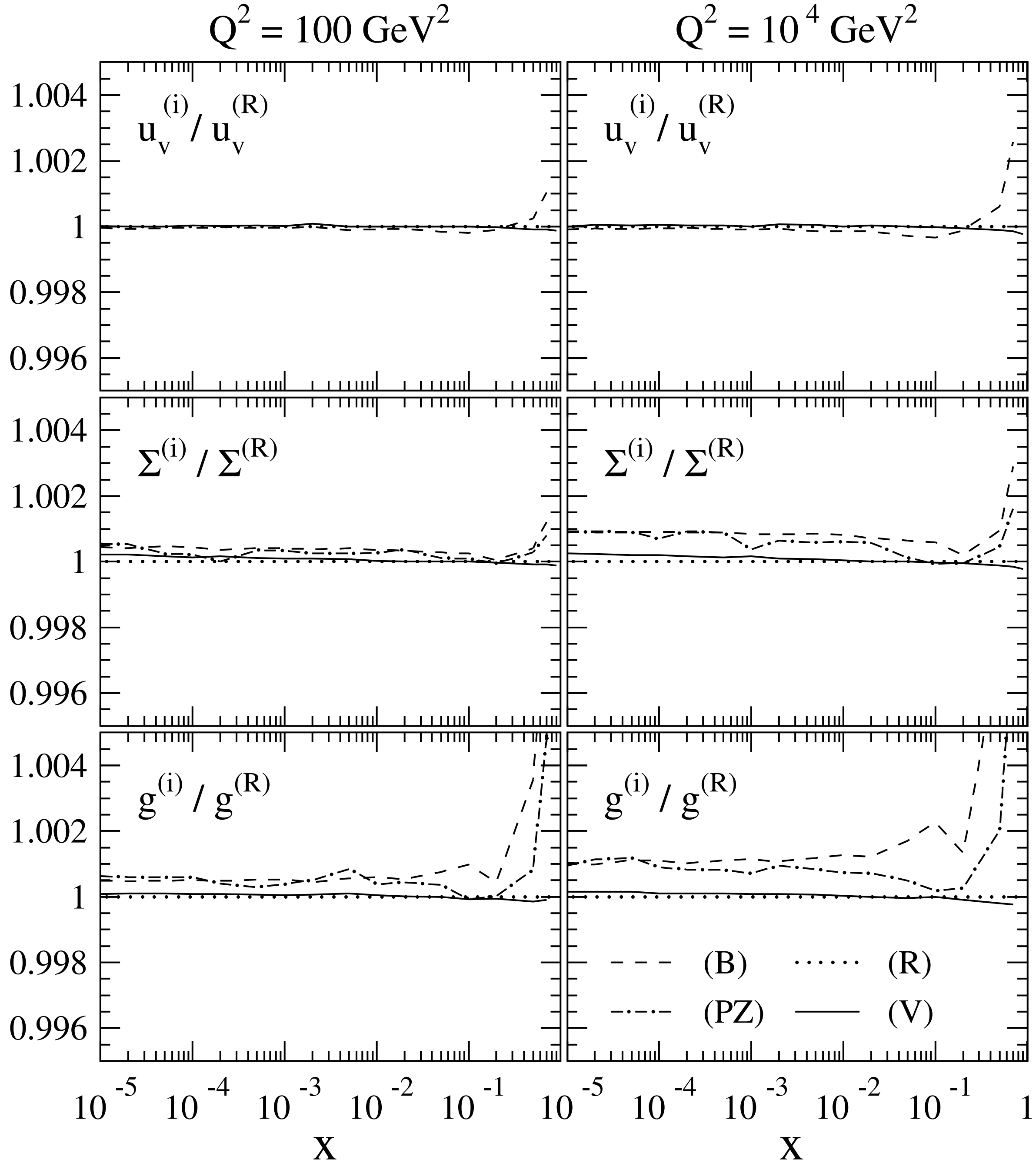


Figure 3: The remaining numerical $x$-dependent deviations on $u_v$, $\Sigma$ and $g$ at $Q^2 = 100$ and $10^4$ GeV$^2$ between the programs of refs. [9, 10, 14, 15], after the differing theoretical assumptions have been corrected for, see the text. The results have been normalized to those of ref. [15].

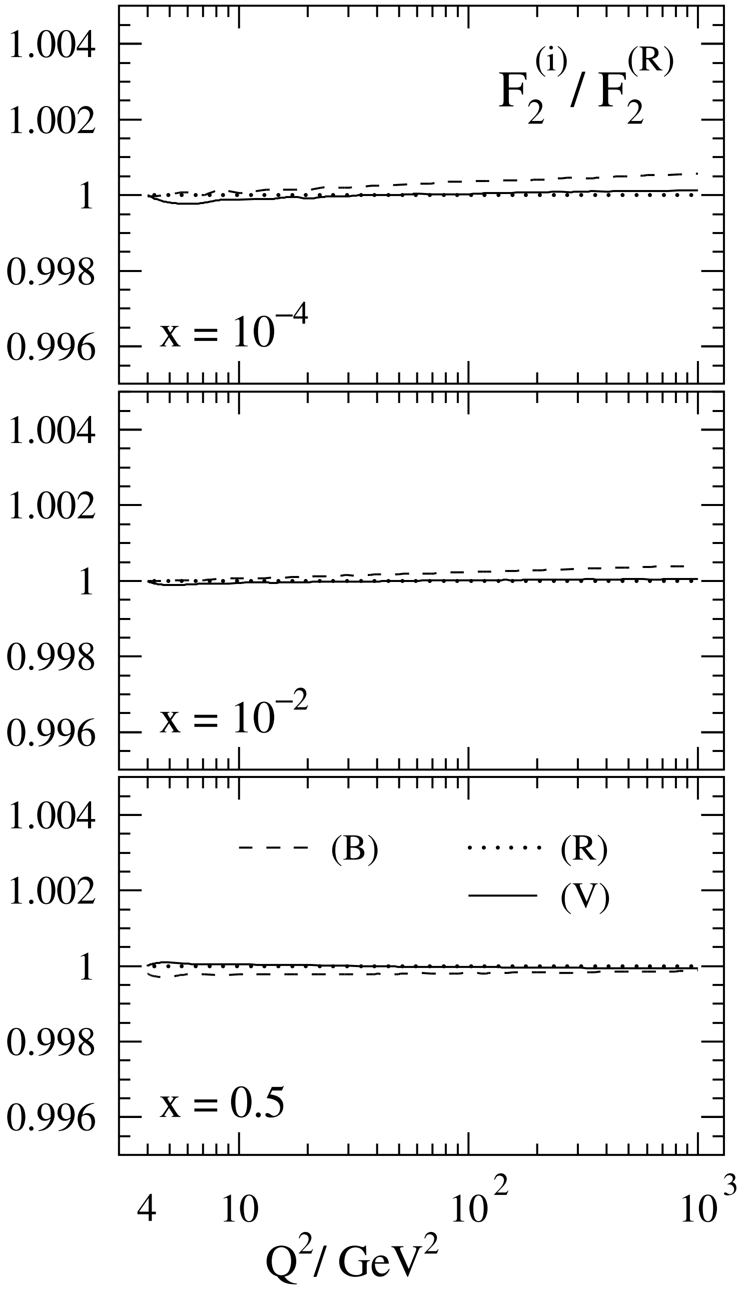


Figure 4: The residual relative offsets in the $Q^2$ evolution of $F_2$ between the programs of refs. [9, 14, 15], after removing the effects due to the different theoretical NLO prescriptions, for three typical values of $x$. As in all previous figures, the initial distributions are taken from eq. (7).

**Acknowledgements :**

We thank R.G. Roberts and W.K. Tung for providing the numerical results of the evolution of our test input with their programs. This work was supported on part by the EC Network 'Human Capital and Mobility' under contract No. CHRX–CT923–0004 and by the German Federal Ministry for Research and Technology (BMBF) under No. 05 7WZ91P (0).

# References

[1] M. Botje, M. Klein, and C. Pascaud, these proceedings.

[2] see e.g. J. Blümlein, in: Proc. of the XXV International Symposium on Multiparticle Dynamics, Stara Lesna, Slovakia, 11–17 September, 1995, eds. D. Bruncko, L. Sandor, and J. Urban, (World Scientific, Singapore, 1996), `hep-ph/9512272`.

[3] W.K. Tung, Nucl. Phys. **B315** (1989) 378.

[4] A.C. Benvenuti et al., BCDMS collaboration, Phys. Lett. **B195** (1987) 97.

[5] W.L. van Neerven, these proceedings, and references therein.

[6] J. Blümlein, S. Riemersma, W.L. van Neerven, and A. Vogt, DESY 96–172, `hep-ph/9609217`, Proceedings of the Workshop 'QCD and QED in Higher Orders', Rheinsberg, Germany, April 1996, eds. J. Blümlein, F. Jegerlehner, and T. Riemann (Nucl. Phys. **B** (Proc. Suppl.) **51C**, 1996) p. 96.

[7] J. Blümlein, S. Riemersma, W.L. van Neerven, and A. Vogt, these proceedings.

[8] M. Virchaux and A. Ouraou, DPhPE 87–15;
M. Virchaux, Thèse, Université Paris-7 (1988);
A. Ourau, Thèse, Université Paris-11 (1988).

[9] M. Botje, QCDNUM15: A fast QCD evolution program, write-up in preparation.

[10] C. Pascaud and F. Zomer, H1 Note `H1-11/94-404`.

[11] M. Diemoz, F. Ferroni, E. Longo, and G. Martinelli , Z. Phys. **C39** (1988) 21.

[12] M. Glück, E. Reya, and A. Vogt, Z. Phys. **C48** (1990) 471.

[13] W. Furmanski and R. Petronzio, Z. Phys. **C11** (1982) 293.

[14] A. Vogt, unpublished.

[15] S. Riemersma, unpublished.

[16] R.G. Roberts, contributed to this workshop.

[17] W.K. Tung, contributed to this workshop.

[18] J. Blümlein and W.L. van Neerven, unpublished. For a short description, see Section 2.4 of ref. [6].